Pakistan Veterinary Journal

ISSN: 0253-8318 (PRINT), 2074-7764 (ONLINE)
DOI: 10.29261/pakvetj/2026.111

RESEARCH ARTICLE

Molecular Identification and Mitochondrial Genome Analysis of Tapeworms in Yaks and Sheep from the Tibetan Plateau

Bin Shi[1]*, Ruihao Hao[2], Qiang Zhang[3] and Qipeng Lv[4]

[1]Key Laboratory of Animal Parasitology of Xizang, Institute of Animal Husbandry and Veterinary Medicine, Xizang Academy of Agricultural and Animal Husbandry Sciences, Lhasa 850009, China; [2]Key Laboratory of Echinococcosis Control, Xizang Agricultural and Animal Husbandry University, Linzhi 860000, China; [3]Agriculture, Rural Affairs, Water Resources and Science & Technology Bureau of Lixian County, Aba Tibetan and Qiang Autonomous Prefecture, Sichuan Province, Li County 623100, China; [4]Xining Wildlife Park, Xining 810000, China
*Corresponding author: sapstone@163.com

ARTICLE HISTORY (26-276)

Received: March 27, 2026
Revised: May 25, 2026
Accepted: May 28, 2026
Published online: May 30, 2026

Key words:
18S rRNA Gene
Mitochondrial Genome
Ruminant Cestodes
Molecular Phylogeny

ABSTRACT

This study aimed to systematically identify cestode species infecting plateau livestock in northern Xizang and characterize their mitochondrial genomes through molecular approaches, providing scientific insights for regional disease control and parasite evolutionary research. Cestode specimens were collected from the small intestines of yaks and sheep in northern Xizang. Phylogenetic analysis was conducted using 18S rRNA gene amplification and sequencing. Whole mitochondrial genomes were sequenced, assembled and annotated via next-generation sequencing (NGS), followed by comprehensive analysis of genomic architecture, nucleotide composition, and evolutionary patterns. Phylogenetic reconstruction revealed that samples T2-2, T2-2-1, T3-2, N1, N2, and N6 clustered closest to *Moniezia* spp. (GU817415) with 98% sequence similarity, while T3-2 showed 95% similarity to family Anoplocephalidae. Sample T3-1 was classified within the *Avitellina* spp. Mitochondrial genome analysis identified four circular double-stranded DNA structures (13,561-13,925 bp) containing 12 PCGs, 22 tRNAs, and 2 rRNAs. All genomes exhibited high A+T content (69.31-73.54%) and gene overlaps. Notably, *Moniezia* spp. displayed 1-7 bp overlaps between cox3 and trnH genes, whereas an unprecedented 40 bp overlap between nad4l and nad4 genes was observed in Anoplocephalidae cestodes, indicating species-specific evolutionary adaptations. This study pioneer's mitochondrial genome data for Tibetan plateau cestodes, uncovering substantial genetic diversity and lineage-specific evolutionary traits. The identification of dominant cestode species and their taxonomic status establishes a critical foundation for targeted antiparasitic strategies and mechanistic investigations into cestode adaptation under extreme high-altitude conditions.

To Cite This Article: Shi B, Hao R, Zhang Q and Lv Q, 2026. Molecular identification and mitochondrial genome analysis of tapeworms in yaks and sheep from the Tibetan plateau. Pak Vet J, 46(5): 1242-1253. http://dx.doi.org/10.29261/pakvetj/2026.111

INTRODUCTION

The infections are caused by the members of class Cestoda that can infect both humans and animals and represent a major concern for public health and livestock production, globally (Hasni *et al*., 2020; Zerguine *et al*., 2025). Among these, members of the family Anoplocephalidae, including the genera *Moniezia*, *Thysaniezia*, and *Avitellina*, are important intestinal parasites of ruminants such as sheep, goats and cattle (Al-Otaibi *et al.,* 2021; Kumar and Kaur, 2023). These parasites are primarily parasitic in small intestine of ruminants including goats, deer and camels (Liu *et al.,* 2019). Once infected with these parasites, hosts may experience clinical symptoms including diarrhea, weight loss and anemia, which significantly affect their normal growth and development. In severe cases, the infection can lead to death (Roncoron *et al.,* 2017; Abdollahi *et al.,* 2023). Organic and inorganic components in cystic fluid have a vital role in physiology, metabolism and immune responses mediated by cestodes, infect internal organs of sheep, goat and cattle leading to diseases. Infection with

tapeworms also decreases the level of glycogen in muscle and liver (Pokora and Kwiatkowski, 2004). These types of parasites are widely distributed throughout the world and are particularly prevalent in regions of China such as Xizang, Qinghai and Xinjiang. Therefore, this situation has caused serious economic losses to animal husbandry industry in the country.

Moniezia belongs to the order Cyclophyllidea, family Anoplocephalidae, and genus *Moniezia*, which is primarily represented by two dominant species, *Moniezia (M.) expansa* and *M. benedeni* (Ohtori *et al.,* 2015). This parasite mainly parasitizes the goats, deer, camels and small ruminants. Infection in susceptible hosts cause symptoms such as diarrhea, weight loss, anemia, and delayed growth and development; serious cases may even end in death (Tam *et al.,* 2020; Zhang *et al.,* 2025). *Moniezia* is widely distributed in the world and is a common parasite in the digestive tract of ruminants, causing serious economic losses in pastoral areas of China (Zhang *et al.,* 2025).

Avitellina belongs to the order Cyclophyllidea, family Anoplocephalidae and genus *Avitellina*. This includes four types of tapeworms: *Avitellina (A.) centriunctata*, *A. parva*, *A. taeniata*, and *A. macrocystis*. These tapeworms mainly parasitize the intestines of domesticated and wild ruminant animals such as cattle, sheep, camels, etc., and is distributed worldwide (Ndom *et al.,* 2019).

In the molecular biology, for classification and identification of tapeworms, mitochondrial genes play a crucial role as important molecular genetic markers. A circular double stranded DNA molecule with a length generally exceeding 12kb is the mitochondrial genome of tapeworms (Spotin *et al.,* 2018). The mitochondrial genome typically encodes 36 genes, comprising 22 transfer RNAs (trnH etc), two ribosomal RNAs (12S and 16S), and 12 protein-coding genes. Structurally, the gene arrangement is compact and there is base overlap between genes, reflecting the simplicity of the mitochondrial genome in post protozoa. The phenomenon of gene overlap may stem from long-term evolutionary pressures. All coding genes are located on the heavy chain. The content of AT is higher than that of GC and the atp8 gene is missing. Besides, the amino acid sequence substitution rate of mitochondrial genome protein encoding genes is relatively high (Wey-Fabrizius *et al.,* 2013).

A distinguishing feature of the tapeworm mitochondrial genome is that transcription and replication of all protein coding genes performed unidirectionally. However, the transcription and replication directions of protein coding genes in the mitochondrial genomes of flukes and nematodes are not necessarily the same. In addition, there are no introns, and there may be overlapping regions between protein coding genes, but the overlapping regions are not large. The 18S rRNA gene is highly conserved among cestodes and has been widely used for family and genus level identification (Neov *et al.,* 2021). This conservative marker allows reliable taxonomic assignment with a single PCR, serving as a cost-effective screening tool prior to whole mitogenome sequencing, which provides higher phylogenetic resolution.

In this study, morphological identification, molecular phylogeny and high-throughput sequencing research methods were comprehensively used to classify and identify tapeworms collected from small intestines of yaks and sheep in northern Tibet based on partial sequences of 18S rDNA, to determine their mitochondrial genomes, to sequence and assemble them, and to study their mitochondrial genome structure and nucleotide polymorphism, which provides significant scientific insights into the evolution and diversity of these parasites.

Materials and methods

Samples collection and DNA extraction: In November 2023, samples of *Moniezia* and *Avitellina* were collected from small intestines of yak and sheep in northern Xizang region (Geji County, Ngari Prefecture and Nyainrong County, Nagqu City). The collected tapeworms were packed into the collection tubes and transported to the laboratory for further identification. A total of eight cestode specimens were collected. The samples were stored in collection tubes and transported to the laboratory on ice within 24 hours. All specimens were obtained from slaughtered animals; no animals were sacrificed for this study.

PCR identification: Total genomic DNA was isolated from the cestode specimens using a Tissue DNA Extraction Kit (Hangzhou BEIWO Medical Technology Co., Ltd., Hangzhou, China), strictly following the manufacturer's protocol. DNA was extracted and stored at -20°C until further investigation. PCR primers targeting a partial region of the cestode 18S rRNA gene were designed and subsequently synthesized by Genewiz (Suzhou, China). The primer sequences were 18S-F (5′-GATTTGGTGGTTGGTGGTGC-3′) and 18S-R (5′-CTGACTCGTTGACACCGTCA-3′). 12.50μL of Premix Taq™, 1.00μL of each primer (10.00pmol/L), 1.00μL of genomic DNA template, and 9.50μL of ddH_2O added to make 25.00μL reaction mixture for PCR amplification. The amplification conditions were: 94°C pre denaturation (3 minutes), followed by 35 cycles, 52°C annealing for 30 seconds, 72°C extension for 1 minute, finally, 72°C extension for 10 minutes. After PCR amplification, 5μL of PCR products were taken for 1.00% agarose gel electrophoresis detection. Remaining PCR products were sent to GENEWIZ (Suzhou, China) for sequencing.

All of the 18S rRNA gene sequences were aligned through NCBI BLAST database (https://blast.ncbi.nlm.nih.gov/Blast.cgi?PROGRAM=blastn&PAGE_TYPE=BlastSearch&LINK_LOC=blasthome) to identify tapeworm species. Multiple sequence alignment was conducted by utilizing MAFFT (v7) with the default iterative refinement strategy. The best-fit nucleotide substitution model for each partition was selected via ModelFinder according to the Bayesian Information Criterion. We applied a partitioned analysis scheme to assign independent evolutionary models to different gene regions. Bayesian phylogenetic inference was carried out using MrBayes 3.2. The Markov chain Monte Carlo was run for 2,000,000 generations, with sampling every 1000 generations. Additionally, a phylogenetic tree was constructed with *Echinococcus granulosus* 4 (GenBank accession number: DQ011167) as the outgroup via Neighbor Joining (NJ) method in MEGA

software (Version 11.0). The Kimura 2-parameter pattern was selected for bootstrap testing (repeated 1000 times) to evaluate nodal reliability.

Genome sequencing and assembly of mitochondria: Using Whole Genome shotgun (WGS) method, libraries with different insertion fragments were constructed. On the basis of Illumina NovaSeq sequencing platform, PE (paired end) sequencing was executed by Next Generation Sequencing (NGS) technology on these libraries. Raw data underwent rigorous quality control using fastp and Adapter Removal. Low-quality reads were filtered based on four criteria: (1) removal of adapter sequences; (2) sliding-window quality trimming (Q<20); (3) exclusion of short reads (<50 bp); and (4) removal of reads with excessive ambiguous bases (N≥5). The sequencing depth for all mitochondria genomes was over 1890x, and coverage was over 98.30%.

High-quality clean reads were assembled into contigs using SPAdes and GetOrganelle. Mitochondrial sequences were identified by BLASTn alignment against the NCBI nt database. Use the Bandage software to view the assembly diagram, confirm the acquisition of the circular contig; and map the reads to the circular sequence, with continuous coverage at both ends without any breaks, thereby confirming the circularization (Wick *et al.,* 2015). Final mitochondrial sequences were obtained by correcting the results using Pilon v1.18 (Walker *et al.,* 2014). The complete assembled mitochondrial genome sequences were uploaded to MITOS web server for functional annotation. The genetic code was set to 'invertebrate mitochondrial code (code 5)', while default parameters of MITOS was set (Bernt *et al.,* 2013). Sequence identities were determined using BLASTn. A cutoff of ≥98.00% similarity was used for genus assignment, and ≥95.00% for family assignment, following standard cestode molecular taxonomy. Since the 18S rRNA gene is highly conserved, species-level identification requires >99.50% similarity; therefore, we report only genus or family names.

MATERIALS AND METHODS

Samples collection and DNA extraction: In November 2023, samples of *Moniezia* and *Avitellina* were collected from small intestines of yak and sheep in northern Xizang region (Geji County, Ngari Prefecture and Nyainrong County, Nagqu City). The collected tapeworms were packed into the collection tubes and transported to the laboratory for further identification. A total of eight cestode specimens were collected. The samples were stored in collection tubes and transported to the laboratory on ice within 24 hours. All specimens were obtained from slaughtered animals; no animals were sacrificed for this study.

PCR identification: Total genomic DNA was isolated from the cestode specimens using a Tissue DNA Extraction Kit (Hangzhou BEIWO Medical Technology Co., Ltd., Hangzhou, China), strictly following the manufacturer's protocol. DNA was extracted and stored at -20°C until further investigation. PCR primers targeting a partial region of the cestode 18S rRNA gene were designed and subsequently synthesized by Genewiz (Suzhou, China). The primer sequences were 18S-F (5′-GATTTGGTGGTTGGTGGTGC-3′) and 18S-R (5′-CTGACTCGTTGACACCGTCA-3′). 12.50μL of Premix Taq™, 1.00μL of each primer (10.00pmol/L), 1.00μL of genomic DNA template, and 9.50μL of ddH_2O added to make 25.00μL reaction mixture for PCR amplification. The amplification conditions were: 94°C pre denaturation (3 minutes), followed by 35 cycles, 52°C annealing for 30 seconds, 72°C extension for 1 minute, finally, 72°C extension for 10 minutes. After PCR amplification, 5μL of PCR products were taken for 1.00% agarose gel electrophoresis detection. Remaining PCR products were sent to GENEWIZ (Suzhou, China) for sequencing.

All of the 18S rRNA gene sequences were aligned through NCBI BLAST database (https://blast.ncbi.nlm.nih.gov/Blast.cgi?PROGRAM=blastn&PAGE_TYPE=BlastSearch&LINK_LOC=blasthome) to identify tapeworm species. Multiple sequence alignment was conducted by utilizing MAFFT (v7) with the default iterative refinement strategy. The best-fit nucleotide substitution model for each partition was selected via ModelFinder according to the Bayesian Information Criterion. We applied a partitioned analysis scheme to assign independent evolutionary models to different gene regions. Bayesian phylogenetic inference was carried out using MrBayes 3.2. The Markov chain Monte Carlo was run for 2,000,000 generations, with sampling every 1000 generations. Additionally, a phylogenetic tree was constructed with *Echinococcus granulosus* 4 (GenBank accession number: DQ011167) as the outgroup via Neighbor Joining (NJ) method in MEGA software (Version 11.0). The Kimura 2-parameter pattern was selected for bootstrap testing (repeated 1000 times) to evaluate nodal reliability.

Genome sequencing and assembly of mitochondria: Using Whole Genome shotgun (WGS) method, libraries with different insertion fragments were constructed. On the basis of Illumina NovaSeq sequencing platform, PE (paired end) sequencing was executed by Next Generation Sequencing (NGS) technology on these libraries. Raw data underwent rigorous quality control using fastp and Adapter Removal. Low-quality reads were filtered based on four criteria: (1) removal of adapter sequences; (2) sliding-window quality trimming (Q<20); (3) exclusion of short reads (<50 bp); and (4) removal of reads with excessive ambiguous bases (N≥5). The sequencing depth for all mitochondria genomes was over 1890x, and coverage was over 98.30%.

High-quality clean reads were assembled into contigs using SPAdes and GetOrganelle. Mitochondrial sequences were identified by BLASTn alignment against the NCBI nt database. Use the Bandage software to view the assembly diagram, confirm the acquisition of the circular contig; and map the reads to the circular sequence, with continuous coverage at both ends without any breaks, thereby confirming the circularization (Wick *et al.,* 2015). Final mitochondrial sequences were obtained by correcting the results using Pilon v1.18 (Walker *et al.,* 2014). The complete assembled mitochondrial genome sequences were uploaded to MITOS web server for functional annotation. The genetic code was set to

'invertebrate mitochondrial code (code 5)', while default parameters of MITOS was set (Bernt *et al.,* 2013). Sequence identities were determined using BLASTn. A cutoff of ≥98.00% similarity was used for genus assignment, and ≥95.00% for family assignment, following standard cestode molecular taxonomy. Since the 18S rRNA gene is highly conserved, species-level identification requires >99.50% similarity; therefore, we report only genus or family names.

RESULTS

PCR amplification and phylogenetic tree analysis: PCR amplification of partial 18S rRNA gene from all eight cestode specimens yielded a specific fragment of 543 bp. This fragment length was consistent with the predicted amplicon size (Fig. 1). Based on the 18S rRNA gene sequences, a phylogenetic tree was constructed using MEGA software (Version 11.0), with *Echinococcus granulosus* (GenBank Accession No. DQ011167) selected as the outgroup. Bootstrap support values (based on 1,000 replicates) are shown at the nodes of the phylogenetic tree (Fig. 2). Samples T2-2, T2-2-1, N2, N6, T3-3, and N1, collected from yaks and sheep in Geji and Nyainrong counties of Xizang, exhibited the closest phylogenetic relationship with *Moniezia* spp. (GU817415). Sample T3-2 was most closely related to Anoplocephalidae, while sample T3-1 showed a close affinity to the *Avitellina* spp. (JQ609343). Consequently, the tapeworms parasitizing yaks and sheep in these regions were identified as *Moniezia* spp., *Avitellina* spp., and species within the Anoplocephalidae family.

Mitochondrial genome characterization of *Moniezia* spp. isolate T2-2: The 13,824 bp in length of complete mitochondrial genome of T2-2 isolate was determined. There were 12 protein-coding genes (PCGs), 22 transfer RNA genes (tRNAs) and two ribosomal RNA genes (rRNAs) encodes a total genome of 36 genes. On positive strand all genes are encoded (Fig. 3). The T2-2 mitochondrial genome exhibits a compact arrangement characterized by gene overlaps and intergenic spacers (Table 1). Eight gene overlap regions were observed in the T2-2 mitochondrial gene, namely: cox3/TrnH, nad4l/nad4, trnQ/trnF, trnF/trnM, trnP/trnI, trnI/trnK, nad3/trnS1, cox1/trnT, trnC/rrnS. The overlapping range ranges from 1-40 bp. In addition, 25 intergenic spacers were observed, with its ranging from 1-259 bp. Among them, the interval region between trnY and trnS2 genes is the longest, at 259 bp.

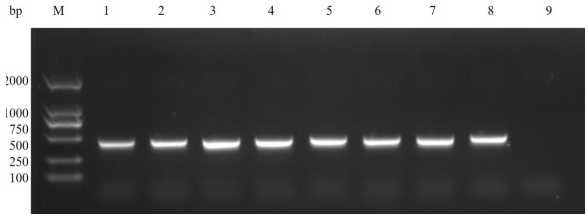

Fig. 1: PCR amplification of the 18S rRNA sequence of cestodes. M: DL2000 DNA marker; 1-8: T2-2、T2-2-1、T3-1、T3-2, T3-3、N1、N2、N6、NC.

The total size of protein encoding genes in T2-2 is 10119 bp, accounting for 73.20% of entire mitochondrial genome. Among them, the cox1 gene is the longest and nad4l is the shortest, and protein encoding genes are similar to those of other *Moniezia* tapeworm proteins. The majority of the starting codons of all protein coding genes are ATG, while TAA and TAG are stop codons. The protein composition consisted of A, T, G, and C at 21.52, 47.79, 22.30 and 8.39%, respectively, with AT-skew and GC-skew values of -0.378 and 0.453. The T2-2 mitochondrial genome was 13,824 bp in length, with nucleotide counts of A=3241, T=6340, G=3025 and C=1218, corresponding to 23.44, 45.86, 21.88 and 8.81%, respectively. A+T proportion (69.31%) was significantly higher than G+C (30.69%).

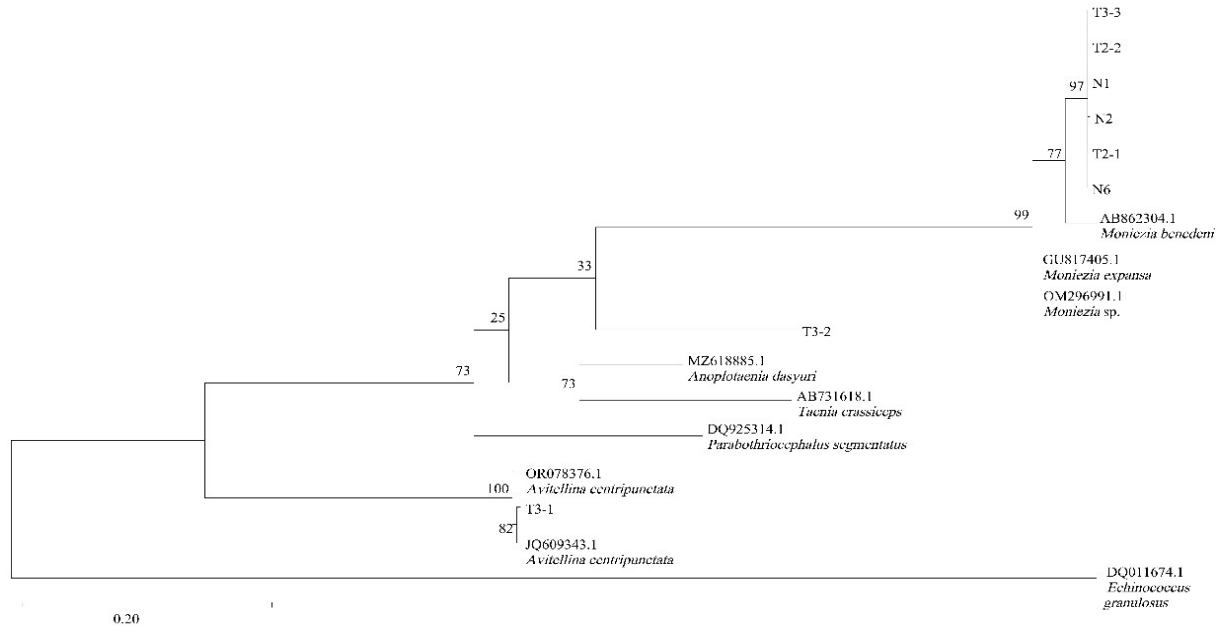

Fig. 2: Phylogenetic tree constructed based on 18S rRNA.

Table 1: Mitochondrial genome structure of *Moniezia* (T2-2)

Feature	Strand	Position	Length (bp)	Initiation codon	Stop codon	Anticodon	Intergenic nucleotide
trnY	+	1-73	73			GTA	259
trnS2	+	333-393	61			TGA	33
trnL1	+	427-494	68			TAG	23
trnL2	+	518-584	67			TAA	42
trnR	+	627-686	60			ACG	3
nad5	+	690-2,267	1578	ATG	TAA		175
trnG	+	2,443-2,505	63			TCC	3
cox3	+	2,509-3,159	651	ATG	TAG		-7
trnH	+	3,153-3,218	66			GTG	4
cob	+	3,223-4,317	1095	ATG	TAA		11
nad4l	+	4,329-4,589	261	ATG	TAG		-40
nad4	+	4,550-5,803	1254	ATG	TAA		
trnQ	+	5,804-5,867	64			TTG	-2
trnF	+	5,866-5,929	64			GAA	-2
trnM	+	5,928-5,994	67			CAT	3
atp6	+	5,998-6,513	516	ATG	TAG		17
nad2	+	6,531-7,406	876	ATG	TAG		1
trnV	+	7,408-7,471	64			TAC	4
trnA	+	7,476-7,541	66			TGC	5
trnD	+	7,547-7,607	61			GTC	3
nad1	+	7,611-8,501	891	GTG	TAG		26
trnN	+	8,528-8,596	69			GTT	8
trnP	+	8,605-8,667	63			TGG	-1
trnI	+	8,667-8,729	63			GAT	2
trnK	+	8,732-8,794	63			CTT	3
nad3	+	8,798-9,145	348	ATG	TAG		-1
trnS1	+	9,145-9,203	59			GCT	3
trnW	+	9,207-9,272	66			TCA	6
cox1	+	9,279-10,892	1614	ATG	TAG		-26
trnT	+	10,867-10,930	64			TGT	
rrnL	+	10,931-11,899	969				
trnC	+	11,900-11,959	60			GCA	-1
rrnS	+	11,959-12,666	708				21
cox2	+	12,688-13,263	576	ATG	TAA		2
trnE	+	13,266-13,329	64			TTC	2
nad6	+	13,332-13,790	459	ATG	TAG		33

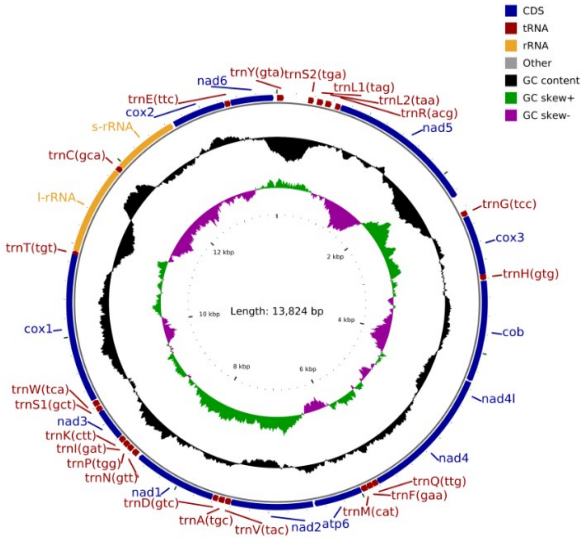

Fig. 3: Mitochondrial gene structure circular diagram of *Moniezia* (T2-2).

Nucleotide skewness analysis showed that relative content of thymine (T) is higher than adenine (A), the AT and GC skew of T2-2 mitochondrial genome are -0.323 and 0.426, respectively. This suggests that in processes such as DNA replication and repair, or due to factors such as selection pressure, T may have a relative advantage in base composition, which may be related to specific functional requirements or evolutionary processes. A higher relative content of G may suggest that this mitochondrial genome region has specificity in recognition of replication origin and chain specific functional exercise (Table 2). tRNA genes total size is 1,428 bp, consisting of 22 tRNAs ranging in length from 59 nucleotides (trnS1) to 71 nucleotides (trnE). Typical cloverleaf structure formed by tRNAs. Anticodons of all other tRNAs start with T or G. The sizes of rrnS (12S) and rrnL (16S) are 764 and 988 bp, respectively. The trnT and trnC make 16S rRNA, but 12S rRNA located between trnC and cox2. 16S rRNA has less A+T content (70.25%) than 12S rRNA (74.87%) (Fig 4).

Mitochondrial genome characterization of *Moniezia* spp. isolate T3-3: The T3-3 isolate has an approximate length of 13,925 bp of complete mitochondrial genome. Annotation of genome revealed two rRNAs, 22 tRNAs, and 12 protein-coding genes (PCGs) making total of 36 genes. Consistent with typical cestode mitochondrial architectures, all genes are exclusively encoded on positive strand (Fig. 4).

Analysis of T3-3 genome organization revealed nine gene overlapping regions, including cox3/trnH, nad4L/nad4, trnQ/trnF, trnF/trnM, trnM/atp6, trnP/trnI, nad3/trnS1, cox1/trnT and trnC/rrnS, with overlap lengths ranging from 1-40 bp. Furthermore, 24 intergenic spacers were identified (1-271 bp), the most significant of which is a 271 bp spacer located between nad5 and trnG. The entire mitochondrial genome accounts for 72.65% of total size of protein-coding genes (PCGs) (10,116 bp). The cox1 gene is the longest, while nad4L is the shortest. ATG and GTG are sued as start codons, while TAA and TAG are used as stop codons (Table 3).

Table 2: Nucleotide composition of the mitochondrial genome of *Moniezia* (T2-2)

Region	A%	C%	G%	T%	A+T%	G+C%	AT skew	GC skew
Whole genome	23.44	8.81	21.88	45.86	69.31	30.69	-0.323	0.426
nad5	25.6	8.75	18.63	47.02	72.62	27.38	-0.295	0.361
cox3	20.74	7.22	24.12	47.93	68.66	31.34	-0.396	0.539
cob	22.28	10.78	21.19	45.75	68.04	31.96	-0.345	0.326
nad4l	22.99	6.51	19.16	51.34	74.33	25.67	-0.381	0.493
nad4	21.37	8.69	22.81	47.13	68.5	31.5	-0.376	0.448
atp6	22.67	10.27	20.16	46.9	69.57	30.43	-0.348	0.325
nad2	17.12	6.05	22.95	53.88	71	29	-0.518	0.583
nad1	19.53	6.96	25.36	48.15	67.68	32.32	-0.423	0.569
nad3	17.82	7.18	24.43	50.57	68.39	31.61	-0.479	0.545
cox1	20.38	9.67	24.1	45.85	66.23	33.77	-0.384	0.428
rrnL	27.49	10.06	20.5	41.95	69.44	30.56	-0.208	0.342
rrnS	28.53	10.03	19.49	41.95	70.48	29.52	-0.19	0.321
cox2	25.52	9.9	23.26	41.32	66.84	33.16	-0.236	0.403
nad6	20.26	8.28	21.79	49.67	69.93	30.07	-0.421	0.449

Table 3: Mitochondrial genome structure of *Moniezia* (T3-3)

Feature	Strand	Position	Length (bp)	Initiation codon	Stop codon	Anticodon	Intergenic nucleotide
trnY	+	1-73	73			GTA	259
trnS2	+	333-393	61			TGA	37
trnL1	+	431-498	68			TAG	23
trnL2	+	522-588	67			TAA	42
trnR	+	631-690	60			ACG	3
nad5	+	694-2,271	1578	ATG	TAA		271
trnG	+	2,543-2,605	63			TCC	3
cox3	+	2,609-3,259	651	ATG	TAG		-7
trnH	+	3,253-3,318	66			GTG	4
cob	+	3,323-4,417	1095	ATG	TAA		12
nad4l	+	4,430-4,690	261	ATG	TAG		-40
nad4	+	4,651-5,904	1254	ATG	TAA		
trnQ	+	5,905-5,968	64			TTG	-2
trnF	+	5,967-6,030	64			GAA	-2
trnM	+	6,029-6,095	67			CAT	-12
atp6	+	6,084-6,596	513	GTG	TAG		35
nad2	+	6,632-7,507	876	ATG	TAG		1
trnV	+	7,509-7,572	64			TAC	4
trnA	+	7,577-7,642	66			TGC	5
trnD	+	7,648-7,708	61			GTC	3
nad1	+	7,712-8,602	891	GTG	TAG		26
trnN	+	8,629-8,697	69			GTT	8
trnP	+	8,706-8,768	63			TGG	-1
trnI	+	8,768-8,830	63			GAT	2
trnK	+	8,833-8,895	63			CTT	3
nad3	+	8,899-9,246	348	ATG	TAG		-1
trnS1	+	9,246-9,304	59			GCT	3
trnW	+	9,308-9,373	66			TCA	6
cox1	+	9,380-10,993	1614	ATG	TAG		-26
trnT	+	10,968-11,031	64			TGT	
rrnL	+	11,032-12,000	969				
trnC	+	12,001-12,060	60			GCA	-1
rrnS	+	12,060-12,767	708				21
cox2	+	12,789-13,364	576	ATG	TAA		2
trnE	+	13,367-13,430	64			TTC	2
nad6	+	13,433-13,891	459	ATG	TAG		33

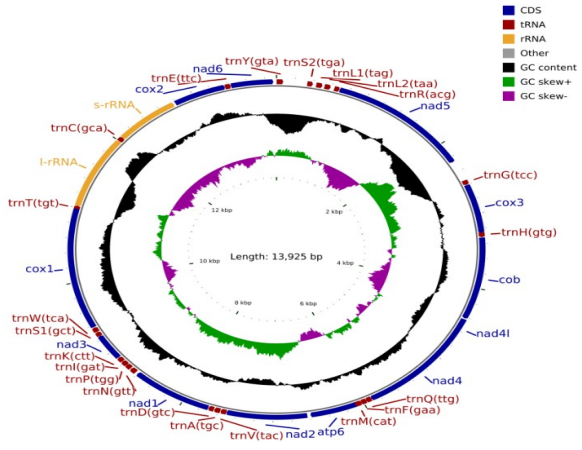

Fig. 4: Circular map of the mitochondrial gene structure of Anoplocephalidae (T3-3).

The nucleotide composition of the T3-3 mitochondrial genome consisted of A, T, C and G at 23.49, 45.90, 8.74 and 21.87%, respectively, with nucleotide counts of 3271, 6392, 1217, and 3045, indicating a significant A+T bias. The A+T content is 69.39%, significantly higher than the G+C content of 30.61%. The AT skew and GC skew of the T3-3 mitochondrial genome were -0.323 and 0.429, respectively. The nucleotide composition of protein-coding genes consisted of A, T, G and C at 21.29, 47.91, 22.41 and 8.39%, respectively. Skewness analysis further showed AT skew (-0.385) and GC skew (0.455), indicating a lower occurrence of adenine and cytosine relative to their complementary bases. The sizes of rrnS (12S) and rrnL (16S) are 708bp and 969bp, respectively. Compositional analysis shows that the A+T content of rrnS (70.48%) is marginally higher than that of rrnL

(69.54%). Notably, these genes are contiguous, separated by no non-coding spacers (Table 4). The total size of the tRNA genes is 1,415 bp, composed of 22 tRNA genes ranging in length from 59 nucleotides (trnS1) to 73 nucleotides (trnY). Only a minority form cloverleaf structure. Except for trnR and trnK, the anticodons of the remaining tRNAs start with T or G.

Mitochondrial genome characterization of the Anoplocephalid isolate T3-2: The T3-2 isolate is 13,719 bp complete mitochondrial genome. Annotation of the sequence identified a total of 36 genes, comprising 12 protein-coding genes, 22 transfer RNAs and two ribosomal RNAs. In addition, genes are present on positive (+) strand (Fig.5). In T3-2 mitochondrial genome, seven gene overlapping regions were observed, specifically: nad4L/nad4, trnF/trnM, atp6/nad2, trnP/trnI, cox1/trnT, cox2/trnE, and nad6/trnY. The overlap ranges varied from 1-34 bp. Additionally, 23 intergenic spacers were observed, ranging from 2-154 bp. Among them, the spacer between trnY and trnS2 was the longest at 154 bp. The 72.65% of entire mitochondrial genome have 10,051 bp. The cox1 gene is the longest, while nad4L is the shortest. Codon usage analysis shows that ATG, TTG and GTG are used as start codons, while TAA and TAG are used as stop codons (Table 5).

The nucleotide composition of T3-2 mitochondrial genome is approximately: A=3,716 (27.09%), T=6,373 (46.45%), G=2,559 (18.65%) and C=1,071 (7.81%). The A+T proportion (73.54%) significantly higher than G+C (26.46%). The AT-skew was -0.263 and GC skew of T3-1 mitochondrial genome was 0.41. This reflects that relative content of thymine (T) is higher than adenine (A). This suggests that T occupies a relative advantage in base composition, likely due to factors such as DNA replication, repair processes, or selection pressure, which may be related to specific functional requirements or evolutionary history. The higher relative G content may imply specificity in replication origin recognition or the execution of strand-specific functions in this mitochondrial genome region. The nucleotide composition of protein-coding genes consisted of A, T, G and C at 24.95, 48.59, 19.32 and 7.14%, respectively, with AT skew (-0.318) and GC skew (0.456) (Table 6).

The 22 transfer RNA (tRNA) genes have combined length of 1,415 bp, with individual size ranging from 59 nt (trnS1) to 73 nt (trnY). The rRNA genes, rrnS (12S) and rrnL (16S) are 708 and 969 bp in length, respectively. In terms of genomic location, rrnS is situated between trnC and cox2, whereas rrnL lies between trnT and trnC. Comparative analysis shows that the A+T content of rrnS (70.48%) is marginally higher than that of rrnL (69.54%).

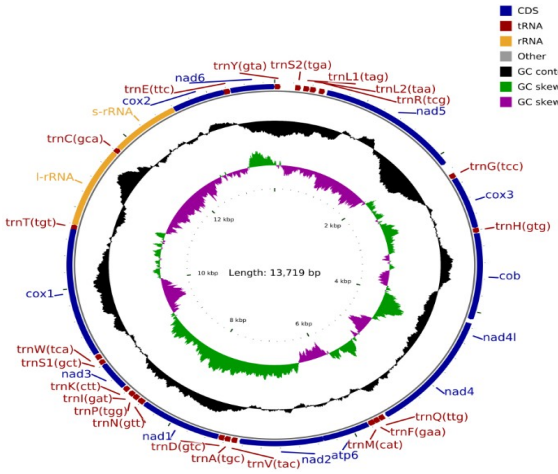

Fig. 5: Circular map of the mitochondrial gene structure of Anoplocephalidae (T3-2).

Mitochondrial genome characterization of *Avitellina* spp. isolate T3-1: The complete mitochondrial genome of *Avitellina* isolate T3-1 was determined to be 13,561 bp in length. Annotation of sequence identified total of 36 genes, comprising 12 PCGs, 22 tRNAs, and two rRNAs. Consistent with the gene arrangement of related cestodes, all genes are present on positive (+) strand (Fig. 6).

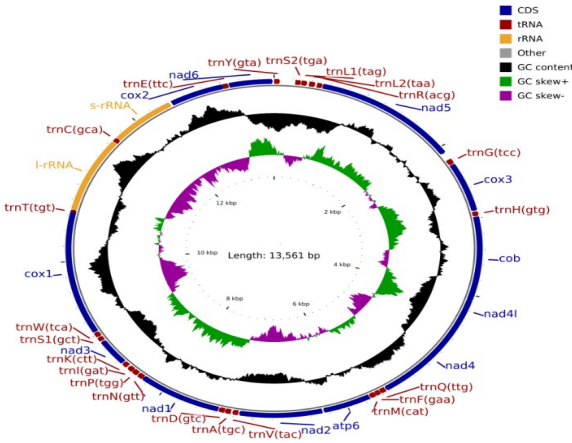

Fig. 6: Circular map of the mitochondrial gene structure of *Avitellina* spp. (T3-1).

Table 4: Nucleotide composition of the mitochondrial genome of *Moniezia* (T3-3)

Region	A%	C%	G%	T%	A+T%	G+C%	AT skew	GC skew
Whole genome	23.49	8.74	21.87	45.9	69.39	30.61	-0.323	0.429
nad5	25.6	8.49	18.63	47.28	72.88	27.12	-0.297	0.374
cox3	20.74	6.91	24.12	48.23	68.97	31.03	-0.399	0.554
cob	22.19	10.59	21.28	45.94	68.13	31.87	-0.349	0.335
nad4l	22.99	6.51	19.16	51.34	74.33	25.67	-0.381	0.493
nad4	21.37	8.77	22.81	47.05	68.42	31.58	-0.375	0.444
atp6	22.03	10.14	21.05	46.78	68.81	31.19	-0.36	0.35
nad2	16.89	5.82	23.17	54.11	71	29	-0.524	0.598
nad1	19.87	7.3	24.92	47.92	67.79	32.21	-0.414	0.547
nad3	17.82	7.47	24.43	50.29	68.1	31.9	-0.477	0.532
cox1	20.14	9.67	24.29	45.91	66.05	33.95	-0.39	0.431
rrnL	27.49	9.96	20.5	42.05	69.54	30.46	-0.209	0.346
rrnS	28.53	10.03	19.49	41.95	70.48	29.52	-0.19	0.321
cox2	25.52	10.07	23.26	41.15	66.67	33.33	-0.234	0.396
nad6	20.26	8.93	21.79	49.02	69.28	30.72	-0.415	0.418

In the genome organization of isolate T3-1, eight gene overlapping regions were observed within the mitochondrial genes, specifically: cob/nad4L, nad4L/nad4, trnF/trnM, nad1/trnN, trnP/trnI, cox1/trnT, trnC/rrnS, and cox2/trnE. The overlap ranges varied from 1-40 bp. Additionally, 24 intergenic spacers were observed, ranging from 2-160 bp. Among them, the spacer between trnY and trnS2 was the longest at 160 bp. The 12 protein-coding genes (PCGs) encompass a cumulative length of 10,119 bp, constituting 73.20% of the total genome. Similar to *Moniezia* spp., cox1 is the largest gene, whereas nad4L is the smallest. Codon usage analysis indicates that the majority of PCGs utilize ATN initiation codons. ATG and GTG are used as start codons, while TAA and TAG are used as stop codons (Table 7).

The nucleotide sequence of the T3-1 mitochondrial genome is 13,561 bp, with A=3,431 (25.31%), T=6,150 (45.35%), G=2,781 (20.51%) and C=1,197 (8.83%). The proportion of A+T (70.66%) is significantly higher than G+C (29.34%). GC and AT-skew of T3-1 mitochondrial genome are 0.398 and -0.284, respectively. This suggests that T and G occupy a relative advantage in base composition.

The nucleotide composition of protein-coding genes consisted of A, T, G and C at 24.19, 47.16, 20.63 and 8.02%, respectively, with AT-skew (-0.321) and GC-skew (0.446). The total size of the tRNA genes is 1,423 bp, ranging in length from 60 nucleotides (trnS1) to 72 nucleotides (trnG). The sizes of rrnS (12S) and rrnL (16S) are 713 bp and 977 bp, respectively. The A+T content of 12S rRNA (70.27%) is slightly higher than that of 16S rRNA (67.76%), and there are no non-coding regions (Table 8). Most of them form the typical cloverleaf structure. With the exception of trnR and trnM, the anticodons of all other tRNAs start with T or G.

Table 5: Mitochondrial genome structure of Anoplocephalidae (T3-2)

Feature	Strand	Position	Length (bp)	Initiation codon	Stop codon	Anticodon	Intergenic nucleotide
trnY	+	1-64	64			GTA	154
trnS2	+	219-281	63			TGA	26
trnL1	+	308-372	65			TAG	7
trnL2	+	380-444	65			TAA	32
trnR	+	477-539	63			TCG	25
nad5	+	565-2,124	1560	TTG	TAA		135
trnG	+	2,260-2,324	65			TCC	3
cox3	+	2,328-2,972	645	ATG	TAG		
trnH	+	2,973-3,034	62			GTG	4
cob	+	3,039-4,104	1066	ATG	T(AA)		45
nad4l	+	4,150-4,410	261	ATG	TAG		-34
nad4	+	4,377-5,612	1236	GTG	TAA		20
trnQ	+	5,633-5,697	65			TTG	
trnF	+	5,698-5,761	64			GAA	-4
trnM	+	5,758-5,826	69			CAT	3
atp6	+	5,830-6,345	516	ATG	TAA		-4
nad2	+	6,342-7,238	897	TTA	TAA		23
trnV	+	7,262-7,325	64			TAC	10
trnA	+	7,336-7,399	64			TGC	2
trnD	+	7,402-7,467	66			GTC	2
nad1	+	7,470-8,360	891	GTG	TAG		6
trnN	+	8,367-8,441	75			GTT	5
trnP	+	8,447-8,511	65			TGG	-1
trnI	+	8,511-8,574	64			GAT	17
trnK	+	8,592-8,654	63			CTT	6
nad3	+	8,661-9,008	348	GTG	TAA		3
trnS1	+	9,012-9,070	59			GCT	10
trnW	+	9,081-9,147	67			TCA	6
cox1	+	9,154-10,737	1584	ATG	TAG		-10
trnT	+	10,728-10,791	64			TGT	
rrnL	+	10,792-11,779	988				
trnC	+	11,780-11,840	61			GCA	
rrnS	+	11,841-12,604	764				
cox2	+	12,605-13,178	574	ATG	T(AA)		-6
trnE	+	13,173-13,243	71			TTC	3
nad6	+	13,247-13,719	473	TTA	TT(A)		-1

Table 6: Nucleotide composition of the mitochondrial genome of Anoplocephalidae (T3-2)

Region	A%	C%	G%	T%	A+T%	G+C%	AT-skew	GC-skew
Whole genome	27.09	7.81	18.65	46.45	73.54	26.46	-0.263	0.41
nad5	30.32	7.76	14.87	47.05	77.37	22.63	-0.216	0.314
cox3	25.12	6.67	20.62	47.6	72.71	27.29	-0.309	0.511
cob	23.83	8.82	18.95	48.41	72.23	27.77	-0.34	0.365
nad4l	23.75	5.75	20.31	50.19	73.95	26.05	-0.358	0.559
nad4	25.32	7.28	18.28	49.11	74.43	25.57	-0.32	0.43
atp6	25.19	8.53	16.47	49.81	75	25	-0.328	0.318
nad2	21.63	6.35	19.84	52.17	73.8	26.2	-0.414	0.515
nad1	19.98	6.4	23.79	49.83	69.81	30.19	-0.428	0.576
nad3	21.26	5.46	21.26	52.01	73.28	26.72	-0.42	0.591
cox1	23.17	9.28	20.71	46.84	70.01	29.99	-0.338	0.381
rrnL	28.95	9.72	19.53	41.8	70.75	29.25	-0.182	0.336
rrnS	32.98	8.9	16.23	41.88	74.87	25.13	-0.119	0.292
cox2	29.62	8.71	20.03	41.64	71.25	28.75	-0.169	0.394
nad6	30.23	4.65	16.7	48.41	78.65	21.35	-0.231	0.564

Table 7: Mitochondrial genome structure of *Avitellina* spp. (T3-1)

Feature	Strand	Position	Length (bp)	Initiation codon	Stop codon	Anticodon	Intergenic nucleotide
trnY	+	1-63	63			GTA	160
trnS2	+	224-286	63			TGA	2
trnL1	+	289-351	63			TAG	18
trnL2	+	370-437	68			TAA	16
trnR	+	454-514	61			ACG	3
nad5	+	518-2,089	1572	ATG	TAA		94
trnG	+	2,184-2,255	72			TCC	3
cox3	+	2,259-2,903	645	ATG	TAG		8
trnH	+	2,912-2,975	64			GTG	4
cob	+	2,980-4,080	1,101	ATG	TAA		-7
nad4l	+	4,074-4,334	261	ATG	TAA		-40
nad4	+	4,295-5,545	1251	ATG	TAA		5
trnQ	+	5,551-5,616	66			TTG	
trnF	+	5,617-5,676	60			GAA	-2
trnM	+	5,675-5,739	65			CAT	3
atp6	+	5,743-6,258	516	ATG	TAA		13
nad2	+	6,272-7,150	879	ATG	TAA		7
trnV	+	7,158-7,221	64			TAC	15
trnA	+	7,237-7,303	67			TGC	
trnD	+	7,304-7,369	66			GTC	4
nad1	+	7,374-8,267	894	GTG	TAG		-1
trnN	+	8,267-8,335	69			GTT	5
trnP	+	8,341-8,407	67			TGG	-1
trnI	+	8,407-8,473	67			GAT	13
trnK	+	8,487-8,551	65			CTT	5
nad3	+	8,557-8,904	348	ATG	TAA		7
trnS1	+	8,912-8,971	60			GCT	4
trnW	+	8,976-9,042	67			TCA	4
cox1	+	9,047-10,648	1602	ATG	TAA		-34
trnT	+	10,615-10,677	63			TGT	
rrnL	+	10,678-11,654	977				
trnC	+	11,655-11,711	57			GCA	-1
rrnS	+	11,711-12,423	713				18
cox2	+	12,442-13,023	582	ATG	TAT		-5
trnE	+	13,019-13,084	66			TTC	3
nad6	+	13,088-13,549	462	ATG	TAG		11

Table 8: Nucleotide composition of the mitochondrial genome of *Avitellina* spp. (T3-1)

Region	A%	C%	G%	T%	A+T%	G+C%	AT skew	GC skew
Whole genome	25.31	8.83	20.51	45.35	70.66	29.34	-0.284	0.398
nad5	24.43	7.32	20.87	47.39	71.82	28.18	-0.32	0.481
cox3	21.71	7.75	23.41	47.13	68.84	31.16	-0.369	0.502
cob	25.34	8.54	20.8	45.32	70.66	29.34	-0.283	0.418
nad4l	27.2	5.36	18.01	49.43	76.63	23.37	-0.29	0.541
nad4	22.78	8.95	20.7	47.56	70.34	29.66	-0.352	0.396
atp6	22.87	8.72	19.77	48.64	71.51	28.49	-0.36	0.388
nad2	24	9.33	18.09	48.58	72.58	27.42	-0.339	0.32
nad1	23.6	7.72	23.27	45.41	69.02	30.98	-0.316	0.502
nad3	24.43	4.89	18.97	51.72	76.15	23.85	-0.358	0.59
cox1	22.78	10.17	21.04	46	68.79	31.21	-0.338	0.348
rrnL	28.66	11.05	21.19	39.1	67.76	32.24	-0.154	0.314
rrnS	28.89	10.38	19.35	41.37	70.27	29.73	-0.178	0.302
cox2	26.46	11.51	23.02	39	65.46	34.54	-0.192	0.333
nad6	23.59	5.19	19.7	51.52	75.11	24.89	-0.372	0.583

Mitogenome-based phylogenetic analysis: To further resolve the phylogenetic position of the four isolates, we constructed a tree based on concatenated mitochondrial protein-coding genes (12 PCGs) using Bayesian inference (Fig. 7). The results of the mitochondrial genome phylogenetic tree show that the isolates T2-2 and T3-3 isolated in this study clearly belong to the Moniezia genus and are similar to the known species *M. benedeni* and *M. expansa*. The isolate T3-2 was identified as Anoplocephalidae. The isolate T3-1 belongs to the Avitellina spp. These results are basically consistent with the 18S results at the genus or family level of classification.

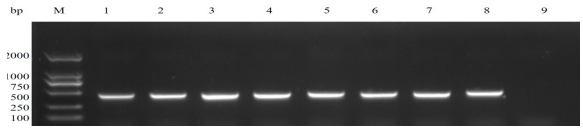

Fig. 1: PCR amplification of the 18S rRNA sequence of cestodes. M: DL2000 DNA marker; 1-8: T2-2, T2-2-1, T3-1, T3-2, T3-3, N1, N2, N6, NC.

DISCUSSION

Cestode infections are among the most important parasitic diseases affecting livestock globally in terms of significant economic losses through reduced productivity and poor animal health (Qamar *et al*., 2025). Members of the family Anoplocephalidae, particularly those of *Moniezia, Thysaniezia* and *Avitellina*, are common intestinal tapeworms of ruminants (Zerguine *et al*., 2025).

Moniezia spp. are large, ribbon-like cestodes (1-5m in length) that inhabit the small intestines of ruminants (Abdelhamid *et al*., 2025). Entire worm body is composed of varying numbers of segments, neck segments and head segments (Muqaddas *et al*., 2024). These parasites possess a highly efficient nutrient absorption mechanism via their tegument and a prolific reproductive capacity, with each proglottid containing multiple sets of reproductive organs. The transmission of *Moniezia* is strictly linked to the seasonal activity of its intermediate host (oribatid mite) (Roczen-Karczmarz and Tomczuk, 2016). Infection occur

when ruminants take cysticercoid larvae and these larvae subsequently develop into adults and parasitize in the small intestine (Abdelhamid *et al*., 2025). The intestinal obstruction, severe catarrhal enteritis, infiltration of eosinophils into lamina propria, and atrophy of intestinal mucosal villi are the pathological damage to host by *Moniezia* spp. (Kumar and Kaur, 2023). More seriously, permanent damage occurs to host when multiple metabolites released from host's immune system and regulated by parasites (Iacob *et al.,* 2020; Yao *et al.,* 2022).

Avitellina spp. are intestinal tapeworms belonging to the class Cestoda, order Cyclophyllidea and family Anoplocephalidae. Its adults parasitize the small intestine of domestic and wild ruminants, and infection may cause serious diarrhea, body failure, reduced weight gain, and intestinal obstruction. In severe cases, lead to death of ruminants (Maizels *et al.,* 2018). The parasite exhibits an indirect life cycle mediated by oribatid mites. Infective cysticercoids harbored Infection occurs when grazing ruminants ingest mites harboring (Ndom *et al.,* 2016). Upon ingestion, larvae excyst, attach to the intestinal mucosa, and mature into adults. Eventually, eggs are disseminated into the environment enclosed within the para-uterine organs of detached gravid proglottids (Otranto *et al.,* 2015). Small ruminants (sheep and goats) are critical global resources for meat, wool, hides and milk, playing a pivotal role in the food security and economy of developing nations. However, the productivity of these animals is severely compromised by gastrointestinal parasitism, particularly in tropical and subtropical regions. Among the Anoplocephalidae, *Avitellina* is one of the most widespread genera. Yet, reliance on morphological characteristics for identification is increasingly challenged, as it frequently results in taxonomic ambiguity, highlighting the need for molecular validation (Kumar and Kaur, 2025).

This study systematically identified the parasitic tapeworm species in yaks and sheep in northern Xizang by integrating morphological and molecular biology methods and mitochondrial genome characteristics of four tapeworms was analyzed, providing important basis for regional tapeworm disease prevention and control as well as tapeworm genetic evolution research. PCR amplification results based on 18S rRNA gene showed that target sequence of 543 bp was successfully obtained from all 8 samples. Subsequent BLAST alignment and phylogenetic analysis revealed distinct clustering patterns: Isolates T2-2 and T2-2-1 exhibited the closest phylogenetic affinity with *Moniezia* spp. (GU817415). Isolate T3-1 formed a clade with *Avitellina* spp. (JQ609343). Isolate T3-2 clustered within the Anoplocephalidae family but remained distinct, suggesting it may represent an unidentified new species or a geographical subspecies (Li *et al.,* 2011). The conservation of 18S rRNA genes makes them an effective marker for classification among distant species. Following standard phylogenetic practice, bootstrap values ≥70% are considered moderate support, and values ≥90% are considered strong support for a given clade. In our tree, the major clades (e.g., clustering of T2-2, T2-2-1, N2, N6, T3-3, N1 with *Moniezia* spp.) received high bootstrap support, indicating reliable relationships (Hong *et al*., 2026). Results further confirmed the reliability of this gene for cestode identification and highlight the genetic diversity of tapeworm populations in Northern Xizang.

The phylogenetic relationships evident from mitochondrial and nuclear markers were highly consistent, demonstrating the reliability of combining multiple molecular markers for cestode taxonomy and evolutionary studies. Multiple studies have likewise confirmed that mitochondrial genomes which provide robust phylogenetic signals for resolving relationships among closely related cestodes and for distinguishing species within *Moniezia* and other related genera (Alshammari *et al*., 2024; Ndiaye *et al*., 2025).

The mitochondrial genome of four cestode species (T2-2, T3-1, T3-2, T3-3) from Northern Xizang were comprehensively sequenced and annotated for the first time. Based solely on 18S rRNA, it is not sufficient to distinguish closely related genera. The mitochondrial genome data provided in this study has higher accuracy. All sample genomes were circular double-stranded DNA, and the mitochondrial genomes of the four cestodes were also circular double-stranded DNA, ranging in length from 13,561 to 13,925 bp. All genomes encode 12 protein-coding genes (PCGs), 22 tRNA genes, and 2 rRNA genes. The gene arrangement is highly conserved, but there are specific gene overlaps and spacer regions and there are species-specific differences: the cox3 and trnH genes of the *Monizia* tapeworm (T2-2, T3-3) overlap (1-7 bp), while the nad4l and nad4 genes of the naked head tapeworm (T3-2) overlap by up to 40 bp, suggesting that it has undergone more significant gene compression during evolution. Although mitochondrial genome and 18S rRNA data provide useful phylogenetic insights, they are insufficient on their own for formal species delimitation. Therefore, the observed genetic differences in this study are interpreted as intraspecific variation or potential population-level divergence rather than evidence of a novel species. A comprehensive integrative taxonomic approach involving additional molecular markers and extensive sampling is required for definitive taxonomic conclusions. The *cox*1 gene sequence phylogenetic analysis from sheep and goat isolates revealed a separate cluster indicated the presence of unique *Coenurus cerebralis* haplotypes in Pakistan. In exploring intraspecific variation due to maternal inheritance, higher evolution rate, high genetic divergence, conserved structure, and absence of recombination, these are important markers (Alvi *et al*., 2020).

The complete mitochondrial genomes obtained in this study ranged from 13,561 to 13,925 bp, which is comparable to previously reported mitochondrial genomes of cestodes. Previous investigations demonstrated that cestode mitochondrial genomes generally contain 36 genes, including 12 protein-coding genes, 22 tRNAs, and two rRNAs, lacking the atp8 gene, which is regarded as a characteristic feature of flatworms (Ndiaye *et al*., 2025). The mitochondrial genomes characterized in this study also exhibited highly compact organizations with extensive gene overlaps and short intergenic spacers, characteristics frequently observed in cestodes and other parasitic helminths. Such compact genomic arrangements may reflect evolutionary pressure toward genome

economization and replication efficiency. Regarding codon usage, while most PCGs use ATG and GTG as the start codon and TAA or TAG as stop codons, suggesting species-specific modifications in genetic codon usage (Tuli *et al.,* 2022). The A+T contents of rrnL (16S rRNA) and rrnS (12S rRNA) range from 67.76-70.75 and 70.27-74.87%, respectively. This composition rich in A+T means that there are fewer hydrogen bonds compared to regions rich in G+C, which may have an important impact on secondary structure stability and ribosomes functional efficiency (Hwang and Kim, 2024).

This study reports the complete mitochondrial genome of tapeworms from the Qinghai-Xizang Plateau for the first time. Although due to the lack of directly comparable reference species genomes, quantitative divergence analysis is currently not possible, we can make several qualitative observations based on the available data. The gene composition (12 PCGs, 22 tRNAs, 2 rRNAs) and gene arrangement (all genes located on the same strand) of the four mitochondrial genomes in this study are consistent with those of other tapeworms of the Cestoda order (such as *M. expansa* and *Avitellina* spp.), indicating that the mitochondrial genome structure of this group has a high degree of evolutionary conservation. Our results show that the overall A+T content (69.31-73.54%) is within the typical range of 65-75% for mitochondrial genomes of protostomes. Gene overlap is relatively common in tapeworm mitochondrial genomes; however, the 40 bp overlap between nad4L and nad4 genes in the isolate T3-2 of the ameboid glandless family is significantly greater than the 1-7 bp overlap typically reported for genes in the *Moniezia* genus and other cestoda tapeworms indicating that this isolate may have undergone genome compression.

All four mitochondrial genomes showed strong A+T nucleotide bias, with A+T content exceeding 69%. Similar nucleotide composition patterns have been reported in numerous cestode mitochondrial genomes, including *M. expansa* and other related anoplocephalid tapeworms. Phylogenetic analyses based on mitochondrial protein-coding genes strongly supported the placement of T2-2 and T3-3 within the genus *Moniezia*, closely related to *M. expansa* and *M. benedeni*. These findings are consistent with already available molecular studies demonstrating significant genetic diversity within *Moniezia* spp. infecting domestic and wild ruminants (Alshammari et al., 2024). Furthermore, the phylogenetic position of isolate T3-1 within *Avitellina* spp. and T3-2 within Anoplocephalidae confirms the coexistence of various cestode lineages in livestock of Xizang.

This study reports mitochondrial genome data of four tapeworms in Northern Xizang, revealing their genetic characteristics and evolutionary relationships. Compared to previous studies, this work addresses the limitations of a single identification method by integrating morphological and molecular data, providing a scientific basis for precise prevention and control of regional tapeworm diseases. However, the limited scope of sample collection and the lack of in-depth exploration of host parasite interaction mechanisms still need improvement. In the future, it is necessary to expand the sampling area, combine transcriptomics and metabolomics to analyze the molecular mechanisms of tapeworms adapting to high-altitude environments, and develop rapid diagnostic techniques based on mitochondrial markers to assist in the sustainable development of animal husbandry.

Conclusions: In conclusion, current study has provided complete mitochondrial genomes and 18S rRNA data for cestode isolates from yaks and sheep in Xizang, improving genetic resources for tapeworms of ruminants. Phylogenetic analyses consistently assigned the isolates to *Moniezia*, *Avitellina* and Anoplocephalidae confirming their taxonomic positions. On the other hand, mitochondrial genomes showed conserved gene order, compact structure and similar codon usage, along with strand-specific nucleotide skew linked to evolutionary constraints. Overall, the results provide a solid molecular framework for identification, classification and understanding of the evolution of ruminant tapeworms, supporting future epidemiological monitoring and control strategies in the region.

Data availability: The raw sequencing data were deposited into the National Genomics Data Center of China under accession number: PRJCA064401 and NCBI GenBank under accession number: PZ428763-PZ428770.

Authors contribution: BS contributed to conceptualization and methodology. BS, RH, QZ, DP, and QL contributed to providing reagents, materials, and analysis tools. BS contributed to writing and preparing the original draft. BS contributed to review and editing. BS contributed to visualization and supervision. All authors reviewed and approved the final manuscript.

Funding: The work was supported by the Base and Talent Project of the Science and Technology Program of Xizang, China (XZ202502JD0028), and the National Key Research and Development Program Project (2022YFE0108100).

Ethics Approval: All procedures performed in this research were approved by the Laboratory Animal Welfare and Ethics Committee of Xizang Academy of Agricultural and Animal Husbandry Sciences (XAAA2025000206). All specimens were collected from slaughtered animals, no animals were sacrificed for this study.

Competing interests: The authors declare no conflict of interest.

Generative AI Statement: No generative artificial intelligence was used in the writing, data analysis, figure generation, or any other aspect of this manuscript. All content is original and authored solely by the named contributors.

REFERENCES

Abdelhamid M, Selim AM, Mohamed RH, *et al*., 2025. Moniezia benedeni infected Zaraibi (Egyptian Nubian) goats: Insights into serum biochemical changes, redox imbalance, and molecular mechanisms of oxidative-inflammatory cascades mediated intestinal injury. Research in Veterinary Science 193:105781.

Abdollahi M, Lotfollahzadeh S, Shokrpoor S, *et al*., 2023. Acute cysticercosis caused by *Cysticercus tenuicollis* in lambs. Journal of Veterinary Internal Medicine 37:1614-1618.

Al-Otaibi BO, Degheidy NS and Al-Malki JS, 2021. Prevalence, incidence and molecular characterization of tape worms in Al Taif governorate, KSA and the effectiveness of *Spirulina platensis* as a biological control *in vitro*. Saudi Journal of Biological Sciences 28:6272-6278.

Alshammari A, Ali U, Kabli AM, *et al*., 2024. Global scenario of genetic diversity in cox1 and nad1 genes of *Moniezia expansa*. Parasite Epidemiology and Control 24.

Alvi MA, Ohiolei JA, Saqib M, *et al*., 2020. First report on molecular characterization of *Taenia multiceps* isolates from sheep and goats in Faisalabad, Pakistan. Frontiers in Veterinary Science 7:594599.

Bernt M, Donath A, Jühling F, *et al*., 2013. MITOS: improved *de novo* metazoan mitochondrial genome annotation. Molecular Phylogenetics and Evolution 69:313-319.

Hasni MS, Khan MK, Imran M, *et al*., 2020. Sero-prevalence of hydatidosis in camel population in different ecological zones of Balochistan Province, Pakistan. International Journal of Agriculture and Biology 24:366-370.

Hong P, Yu S, Liu TC, *et al*., 2026. Molecular characterization of *Moniezia expansa* (Rudolphi, 1810) (Cestoda: Anoplocephalidae) from a captive common eland (*Tragelaphus oryx*) in Taiwan. International Journal for Parasitology: Parasites and Wildlife p.101220.

Hwang HJ and Kim YK, 2024. Molecular mechanisms of circular RNA translation. Experimental & Molecular Medicine 56:1272-1280.

Iacob OC, El-Deeb WM, Paşca SA, *et al*., 2020. Uncommon co-infection due to *Moniezia expansa* and *Moniezia benedeni* in young goats from Romania: morphological and histopathological analysis. Annals of Parasitology 66:501-507.

Kumar S and Kaur H, 2023. Molecular characterization of *Avitellina lahorea* Woodland, 1927 (Class Cestoda; Family Anoplocephalidae) infecting sheep and goats raised in India. Acta Parasitologica 68:359-371.

Kumar S and Kaur H, 2023. Molecular characterization of *Moniezia denticulata* (Rudolphi, 1810) and its distinction from *M. expansa* infecting sheep and goats raised in the north and north-western regions of India. Parasitology 150:831-841.

Kumar S and Kaur H, 2025. Taxonomy of the cestodes *Avitellina sudanea* and *A. centripunctata* (Cyclophyllidea, Thysanosomatidae) parasitic in sheep and goats in India based on morphological and molecular evidence. Systematic Parasitology 102:36.

Li Y, Liu H and Yang YM, 2011. Application of molecular biological techniques in *Taenia* identification. Chinese Journal of Parasitology & Parasitic Diseases 29:385-388.

Liu Y, Wang Z, Pang S, *et al*., 2019. Evaluation of dynamic developmental processes and the molecular basis of the high body fat percentage of different proglottid types of *Moniezia expansa*. Parasites & Vectors 12:390.

Maizels RM, Smits HH and McSorley HJ, 2018. Modulation of host immunity by helminths: The expanding repertoire of parasite effector molecules. Immunity 49:801-818.

Muqaddas H, Mehmood N, Nigar M, *et al*., 2024. First molecular report of *Moniezia expansa* in small ruminants of Pakistan with epidemiological insight. PLoS One 19.

Ndiaye MP, Ndom M, Kénémé B, *et al*., 2025. Diversity and phylogenetic relationships among *Moniezia* spp. (Cestoda: Anoplocephalidae): An inference from COX1 and SSU rDNA sequences. African Journal of Parasitology, Mycology and Entomology 3:7.

Ndom M, Diop G, Quilichini Y, *et al*., 2016. Prevalence and scanning electron microscopic identification of anoplocephalid cestodes among small ruminants in Senegal. Journal of Parasitology Research 2016:3937292.

Ndom M, Diop G, Yanagida T, *et al*., 2019. Morphological and genetic characterizations of *Avitellina* tapeworms from domestic ruminants in Senegal: An evidence of specificity among sheep and cattle host. Veterinary Parasitology, Regional Studies and Reports 18:100337.

Neov B, Vasileva GP, Radoslavov G, *et al*., 2021. Phylogeny of hymenolepidids (Cestoda: Cyclophyllidea) from mammals: sequences of 18S rRNA and COI genes confirm major clades revealed by the 28S rRNA analyses. Journal of Helminthology 95.

Ohtori M, Aoki M, Itagaki TJJ, *et al*., 2015. Sequence differences in the internal transcribed spacer 1 and 5.8 S ribosomal RNA among three *Moniezia* species isolated from ruminants in Japan. Journal of Veterinary Medical Science 77:105-107.

Otranto D, Cantacessi C, Dantas-Torres F, *et al*., 2015. The role of wild canids and felids in spreading parasites to dogs and cats in Europe. Part II: Helminths and arthropods. Veterinary Parasitology 213:24-37.

Pokora Z and Kwiatkowski S, 2004. Glycogen level in the liver and skeletal muscles of bream (*Abramis brama*) infected with plerocercoids of *Ligula intestinalis* (Cestoda: Pseudophyllidea). Archives of Environmental Protection 113-119.

Qamar W, Abbas RZ, Imran M, *et al*., 2025. Prevalence and associated risk factors of *Cysticercus tenuicollis* in the small ruminants in different districts of Punjab and KPK Provinces of Pakistan. Journal of Animal and Plant Sciences 35:935-945.

Roczen-Karczmarz M and Tomczuk K, 2016. Oribatid mites as vectors of invasive diseases. Acarologia 56:613-623.

Roncoron C, Fagiolo A, Amoruso C, *et al*., 2017. *Anoplocephala* sp. (Cestoda, Cyclophyllidea) infection in horses in Central Italy. Veterinaria Italiana 53:85-87.

Spotin A, Boufana B, Ahmadpour E, *et al*., 2018. Assessment of the global pattern of genetic diversity in *Echinococcus multilocularis* inferred by mitochondrial DNA sequences. Veterinary Parasitology 262:30-41.

Tam TT, Lan NTK and Doanh PN, 2020. Morphological differences and molecular phylogenetic relationship of two tapeworm species, *Moniezia expansa* and *Moniezia benedeni*, collected from domestic ruminants in northern Vietnam. Parasitology International 74:101998.

Tuli MD, Li H, Pan X, *et al*., 2022. Heteroplasmic mitochondrial genomes of a *Raillietina* tapeworm in wild pangolin. Parasites & Vectors 15:204.

Walker BJ, Abeel T, Shea T, *et al*., 2014. Pilon: an integrated tool for comprehensive microbial variant detection and genome assembly improvement. PLoS One 9.

Wick RR, Schultz MB, Zobel J, *et al*., 2015. Bandage: interactive visualization of *de novo* genome assemblies. Bioinformatics 31:3350-3352.

Yao WL, Liu LP, Wen YQ, *et al*., 2022. *Moniezia benedeni* infection enhances neuromedin U (NMU) expression in sheep (*Ovis aries*) small intestine. BMC Veterinary Research 18:143.

Zerguine K, Meryem B, Imane D, *et al*., 2025. Prevalence, risk factors and morphological description of intestinal cestodes of small ruminants in Algeria. Biologia 80:1323-1334.

Zhang S, Zhao Y, Liang W, *et al*., 2025. Rapid visual detection of *Moniezia* spp. in sheep feces via Recombinase Polymerase Amplification-Lateral Flow Dipstick (RPA-LFD) assay. Veterinary Parasitology 339:110582.